

Search for Exclusive Multi-body Non- $D\bar{D}$ Decays at the $\psi(3770)$

G. S. Huang,¹ D. H. Miller,¹ V. Pavlunin,¹ B. Sanghi,¹ I. P. J. Shipsey,¹ G. S. Adams,²
 M. Cravey,² J. P. Cummings,² I. Danko,² J. Napolitano,² Q. He,³ H. Muramatsu,³
 C. S. Park,³ E. H. Thorndike,³ T. E. Coan,⁴ Y. S. Gao,⁴ F. Liu,⁴ M. Artuso,⁵
 C. Boulahouache,⁵ S. Blusk,⁵ J. Butt,⁵ O. Dorjkhaidav,⁵ J. Li,⁵ N. Mena,⁵ R. Mountain,⁵
 R. Nandakumar,⁵ K. Randrianarivony,⁵ R. Redjimi,⁵ R. Sia,⁵ T. Skwarnicki,⁵
 S. Stone,⁵ J. C. Wang,⁵ K. Zhang,⁵ S. E. Csorna,⁶ G. Bonvicini,⁷ D. Cinabro,⁷
 M. Dubrovin,⁷ R. A. Briere,⁸ G. P. Chen,⁸ J. Chen,⁸ T. Ferguson,⁸ G. Tatishvili,⁸
 H. Vogel,⁸ M. E. Watkins,⁸ J. L. Rosner,⁹ N. E. Adam,¹⁰ J. P. Alexander,¹⁰
 K. Berkelman,¹⁰ D. G. Cassel,¹⁰ V. Crede,¹⁰ J. E. Duboscq,¹⁰ K. M. Ecklund,¹⁰
 R. Ehrlich,¹⁰ L. Fields,¹⁰ R. S. Galik,¹⁰ L. Gibbons,¹⁰ B. Gittelman,¹⁰ R. Gray,¹⁰
 S. W. Gray,¹⁰ D. L. Hartill,¹⁰ B. K. Heltsley,¹⁰ D. Hertz,¹⁰ C. D. Jones,¹⁰
 J. Kandaswamy,¹⁰ D. L. Kreinick,¹⁰ V. E. Kuznetsov,¹⁰ H. Mahlke-Krüger,¹⁰
 T. O. Meyer,¹⁰ P. U. E. Onyisi,¹⁰ J. R. Patterson,¹⁰ D. Peterson,¹⁰ E. A. Phillips,¹⁰
 J. Pivarski,¹⁰ D. Riley,¹⁰ A. Ryd,¹⁰ A. J. Sadoff,¹⁰ H. Schwarthoff,¹⁰ X. Shi,¹⁰
 M. R. Shepherd,¹⁰ S. Stroiney,¹⁰ W. M. Sun,¹⁰ D. Urner,¹⁰ T. Wilksen,¹⁰ K. M. Weaver,¹⁰
 M. Weinberger,¹⁰ S. B. Athar,¹¹ P. Avery,¹¹ L. Brevva-Newell,¹¹ R. Patel,¹¹
 V. Potlia,¹¹ H. Stoeck,¹¹ J. Yelton,¹¹ P. Rubin,¹² C. Cawfield,¹³ B. I. Eisenstein,¹³
 G. D. Gollin,¹³ I. Karliner,¹³ D. Kim,¹³ N. Lowrey,¹³ P. Naik,¹³ C. Sedlack,¹³
 M. Selen,¹³ E. J. White,¹³ J. Williams,¹³ J. Wiss,¹³ K. W. Edwards,¹⁴ D. Besson,¹⁵
 T. K. Pedlar,¹⁶ D. Cronin-Hennessy,¹⁷ K. Y. Gao,¹⁷ D. T. Gong,¹⁷ J. Hietala,¹⁷
 Y. Kubota,¹⁷ T. Klein,¹⁷ B. W. Lang,¹⁷ S. Z. Li,¹⁷ R. Poling,¹⁷ A. W. Scott,¹⁷
 A. Smith,¹⁷ S. Dobbs,¹⁸ Z. Metreveli,¹⁸ K. K. Seth,¹⁸ A. Tomaradze,¹⁸ P. Zweber,¹⁸
 J. Ernst,¹⁹ H. Severini,²⁰ D. M. Asner,²¹ S. A. Dytman,²¹ W. Love,²¹ S. Mehrabyan,²¹
 J. A. Mueller,²¹ V. Savinov,²¹ Z. Li,²² A. Lopez,²² H. Mendez,²² and J. Ramirez²²

(CLEO Collaboration)

¹*Purdue University, West Lafayette, Indiana 47907*

²*Rensselaer Polytechnic Institute, Troy, New York 12180*

³*University of Rochester, Rochester, New York 14627*

⁴*Southern Methodist University, Dallas, Texas 75275*

⁵*Syracuse University, Syracuse, New York 13244*

⁶*Vanderbilt University, Nashville, Tennessee 37235*

⁷*Wayne State University, Detroit, Michigan 48202*

⁸*Carnegie Mellon University, Pittsburgh, Pennsylvania 15213*

⁹*Enrico Fermi Institute, University of Chicago, Chicago, Illinois 60637*

¹⁰*Cornell University, Ithaca, New York 14853*

¹¹*University of Florida, Gainesville, Florida 32611*

¹²*George Mason University, Fairfax, Virginia 22030*

¹³*University of Illinois, Urbana-Champaign, Illinois 61801*

¹⁴*Carleton University, Ottawa, Ontario, Canada K1S 5B6*

and the Institute of Particle Physics, Canada

¹⁵*University of Kansas, Lawrence, Kansas 66045*

¹⁶*Luther College, Decorah, Iowa 52101*

¹⁷*University of Minnesota, Minneapolis, Minnesota 55455*

¹⁸*Northwestern University, Evanston, Illinois 60208*

¹⁹*State University of New York at Albany, Albany, New York 12222*

²⁰*University of Oklahoma, Norman, Oklahoma 73019*

²¹*University of Pittsburgh, Pittsburgh, Pennsylvania 15260*

²²*University of Puerto Rico, Mayaguez, Puerto Rico 00681*

(Dated: January 27, 2006)

Abstract

Using data collected at the $\psi(3770)$ resonance with the CLEO-c detector at the Cornell e^+e^- storage ring, we present searches for 25 charmless decay modes of the $\psi(3770)$, mostly multibody final states. No evidence for charmless decays is found.

The $\psi(3770)$ is the lowest-mass charmonium resonance above $D\bar{D}$ threshold [1]. It may be the 1^3D_1 state or a mixture of 1^3D_1 and 2^3S_1 . Charmless decays of the $\psi(3770)$ can shed light on $S - D$ mixing, missing $\psi(2S)$ decays such as $\psi(2S) \rightarrow \rho\pi$, the discrepancy between the total and $D\bar{D}$ cross section at the $\psi(3770)$, and rescattering effects contributing to an enhanced $b \rightarrow s$ penguin amplitude in B meson decays [2].

The total cross section at the $\psi(3770)$ was estimated from older measurements to be (7.9 ± 0.6) nb in [2], which is larger by about 20% than the measured $D\bar{D}$ cross section $(6.39 \pm 0.10^{+0.17}_{-0.08})$ nb [3]. While the significance of the discrepancy between the total cross section and the $D\bar{D}$ cross section is not large, identifying non- $D\bar{D}$ decays of the $\psi(3770)$ will place the discrepancy on a solid footing and shed light on the nature of the $\psi(3770)$. The BES Collaboration observed $\psi(3770) \rightarrow \pi^+\pi^- J/\psi$ with a branching ratio of $(0.34 \pm 0.14 \pm 0.09)\%$ [4], while CLEO measured a branching ratio of $(0.189 \pm 0.022^{+0.007}_{-0.004})\%$ [5]. This non- $D\bar{D}$ channel contributes approximately 100 keV to the $\psi(3770)$ decay width, which motivates the search for other exclusive final states.

Charmless decays of the $\psi(3770)$ may provide an avenue to study rescattering effect relevant to B meson decays. For example, the η' exhibits enhanced production in charmless inclusive and exclusive B meson decays which is not well understood. If the $\psi(3770)$ decays to $D\bar{D}$ pairs which subsequently re-annihilate into non-charmed final states, a similar effect could contribute to enhanced $b \rightarrow s$ penguin amplitudes in B meson decays, including modes containing an η' , i.e. $b \rightarrow c\bar{c}s \rightarrow q\bar{q}s$, where $q = (u, d, s)$.

Although the $\psi(3770)$ is believed to be primarily the 1^3D_1 state of the $c\bar{c}$ system, its large leptonic width indicates mixing with S -wave states, particularly the $\psi(2S)$. By enhancing the rate of non- $D\bar{D}$ decays at the $\psi(3770)$, mixing between the $\psi(3770)$ and the $\psi(2S)$ provides an explanation for the anomalously small $\psi(2S)$ branching fractions to some hadronic 2-body final states such as $\rho\pi$ [2].

In this Letter, we report results of searches for a wide variety of non- $D\bar{D}$ modes, including final states with and without strangeness and with and without baryons. The modes $\eta(^{\prime})3\pi$ are included since recent predictions exist [2]. Modes with baryons are included since any observation would be unambiguously a non- $D\bar{D}$ decay because D mesons are not sufficiently massive to decay to baryon pairs.

The data sample used in this analysis is obtained at the $\psi(3770)$ and the nearby continuum in e^+e^- collisions produced by the Cornell Electron Storage Ring (CESR) and acquired with the CLEO-c detector. The CLEO-c [6] detector is a modification of the CLEO III detector [7], in which the silicon-strip vertex detector was replaced by a six-layer all-stereo drift chamber. The solid angle coverage for charged and neutral particles is 93% of 4π . The charged particle tracking system, operating in a 1.0 T magnetic field directed along the beam axis, achieves a momentum resolution of $\sim 0.6\%$ at $p = 1$ GeV. The calorimeter attains a photon energy resolution of 2.2% at $E_\gamma = 1$ GeV and 5% at 100 MeV. Two particle identification systems, one based on energy loss (dE/dx) in the drift chamber and the other a ring-imaging Cherenkov (RICH) detector, are used together to identify π^\pm , K^\pm and $p(\bar{p})$. The combined dE/dx -RICH particle identification procedure has efficiencies exceeding 90% and misidentification rates below 5% for these three particle species.

The integrated luminosity (\mathcal{L}) of the datasets was measured using e^+e^- , $\gamma\gamma$, and $\mu^+\mu^-$ final states [8]. Event counts were normalized with a Monte Carlo (MC) simulation based on the Babayaga [9] event generator combined with GEANT-based [10] detector modeling. The data consist of $\mathcal{L}=55.8$ pb $^{-1}$ on the peak of the $\psi(3770)$ and 20.70 pb $^{-1}$ at the continuum ($\sqrt{s}=3.67$ GeV), which is used for background subtraction. The nominal scale factor used

to normalize continuum yields to $\psi(3770)$ data is $f_{\text{co}}^{\text{nom}} = 2.55 \pm 0.26$, and is determined from the integrated luminosities of the data sets corrected for an assumed $1/s$ dependence of the cross section where the error is from the uncertainties in the relative luminosity and the s dependence of the cross section. The scale factor differs by a factor of 5.2% for each power of $1/s$. The value of f_{co} used for each mode also corrects for the small difference in efficiency between the $\psi(3770)$ and continuum data.

The analysis strategy and selection criteria are the same as in the CLEO-c analysis of exclusive hadronic decays at the $\psi(2S)$ [11]. Standard requirements are used to select charged particles reconstructed in the tracking system and photon candidates in the CsI calorimeter. We require tracks of charged particles to have momenta $p > 100$ MeV and to satisfy $|\cos\theta| < 0.90$, where θ is the polar angle with respect to the e^+ direction. Each photon candidate satisfies $E_\gamma > 30$ MeV and is more than 8 cm away from the projections of charged tracks into the calorimeter. Particle identification is used for all charged particle candidates. Pions, kaons, and protons must be positively and uniquely identified. That is: pion candidates must not satisfy kaon or proton selection criteria, and kaon and proton candidates obey similar requirements. Charged particles must not be identified as electrons using criteria based on momentum, calorimeter energy deposition, and dE/dx .

The invariant mass of the decay products from the following particles must lie within limits determined from MC studies: π^0 ($120 \leq M_{\gamma\gamma} \leq 150$ MeV), η ($500 \leq M_{\gamma\gamma} \leq 580$ MeV, $530 \leq M_{\pi^+\pi^-\pi^0} \leq 565$ MeV), ω ($740 \leq M_{\pi^+\pi^-\pi^0} \leq 820$ MeV [$760 \leq M_{\pi^+\pi^-\pi^0} \leq 800$ MeV for the $\omega p\bar{p}$ final state]), ϕ ($1.00 \leq M_{K^+K^-} \leq 1.04$ GeV), and Λ ($1.112 \leq M_{p\pi^-} \leq 1.120$ GeV). For $\pi^0 \rightarrow \gamma\gamma$ and $\eta \rightarrow \gamma\gamma$ candidates in events with more than two photons, the combination giving a mass closest to the known π^0 or η mass is chosen, and a kinematically constrained fit to the known parent mass is made [12]. To suppress electromagnetic energy deposits in the calorimeter mimicking a π^0 or η , each electromagnetic shower profile is required to be consistent with that of a photon. For $\eta \rightarrow \pi^+\pi^-\pi^0$ and $\omega \rightarrow \pi^+\pi^-\pi^0$, the π^0 is selected as described above, and then combined with all possible combinations of two oppositely charged pions choosing the combination that is closest to the known $\eta(\omega)$ mass. For $\Lambda \rightarrow p\pi^-$, a fit of the p and π^- trajectories to a common vertex separated from the e^+e^- interaction ellipsoid is made. Contamination from K_S^0 decays is eliminated by particle identification and energy conservation requirements.

Reconstructed events must conserve momentum and energy. The hadrons comprising these events each have momentum p_i and combined measured energy E_{vis} . We require the measured scaled energy $E_{\text{vis}}/E_{\text{cm}}$ be consistent with unity within experimental resolution, which varies by final state. We require $|\Sigma \mathbf{p}_i|/E_{\text{cm}} < 0.02$. Together these requirements suppress backgrounds with missing energy or incorrect mass assignments. The experimental resolutions are smaller than 1% in scaled energy and 2% in scaled momentum.

For the final states with four charged tracks and a π^0 , an additional cut is applied to remove a background of radiative events. When the highest energy photon in an event is combined with a low-energy photon candidate, it can imitate a π^0 . We require $(E_{4\text{tracks}} + E_\gamma)/E_{\text{cm}} < 0.995$, where E_γ is the energy of the highest energy photon. For the final states $2(\pi^+\pi^-)$ and $2(\pi^+\pi^-)\pi^0$, there is a background from $(\gamma)\pi^+\pi^-J/\psi$ arising mostly from radiative returns to the $\psi(2S)$. This background is vetoed if the recoil mass against the two slowest oppositely charged tracks (assumed to be pions), m_2^{slow} , satisfies $3.15 < m_2^{\text{slow}} < 3.22$ GeV, and/or the invariant mass of the two fastest oppositely charged tracks (assumed to be muons unless the dE/dx measurement is consistent with electrons), m_2^{fast} , satisfies $3.05 < m_2^{\text{fast}} < 3.15$ GeV. For the final states $2(\pi^+\pi^-)\pi^0$, $K^+K^-\pi^+\pi^-$ and $K^+K^-\pi^+\pi^-\pi^0$,

in order to remove $D\bar{D}$ background, we exclude events in which the invariant mass of the following combinations of particles is consistent with a D^0/D^\pm meson: $\pi^+\pi^-\pi^0$, $K^\pm\pi^\mp$, $\pi^+\pi^-$, K^+K^- , $K^\pm\pi^\mp\pi^0$, $K^+K^-\pi^0$ or $\pi^\pm\pi^0$.

For every final state, a signal selection range in $E_{\text{vis}}/E_{\text{cm}}$ is determined by Monte Carlo simulation, and a sideband selection range is defined to measure background. The signal range in $E_{\text{vis}}/E_{\text{cm}}$ varies between $0.98 - 1.02$ and $0.99 - 1.01$ depending on the final state. Final states with an intermediate η , ω , or ϕ must satisfy a scaled energy signal selection range requirement identical to the corresponding mode without the intermediate particle, and the event yield is determined from signal and sideband selection ranges of the particle mass. For example, the scaled energy signal selection range is the same for ϕK^+K^- and $K^+K^-K^+K^-$. Most modes studied in this Letter have resonant sub-modes, however, only narrow resonances are included in this analysis.

In Fig. 1, the scaled energy and invariant mass distributions are shown for two typical modes: $2(\pi^+\pi^-)\pi^0$ and $K^+K^-\pi^+\pi^-$. Evidence for production of the ω and ϕ resonances, respectively, is observed in the corresponding mass spectra. The background from $D\bar{D}$ is tiny, and thus is almost invisible.

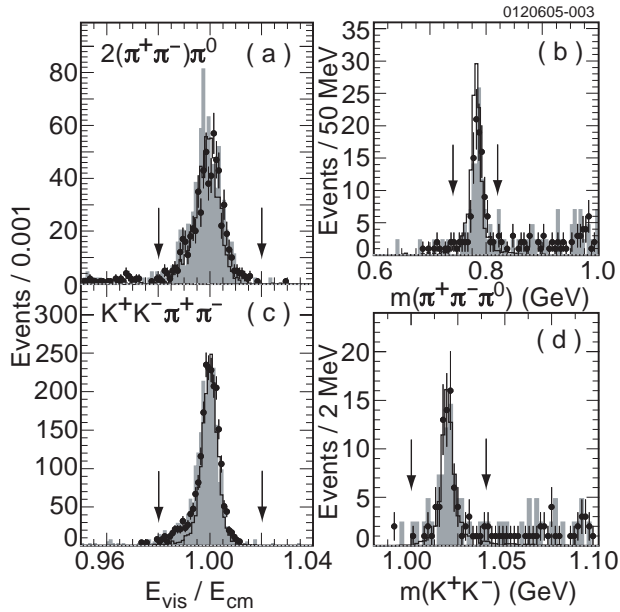


FIG. 1: Distributions for the modes $2(\pi^+\pi^-)\pi^0$ [(a) and (b)], $K^+K^-\pi^+\pi^-$ [(c) and (d)]. The pairs of arrows indicate the signal regions. (a) and (c) The scaled total energy. (b) The $\pi^+\pi^-\pi^0$ invariant mass in $2(\pi^+\pi^-)\pi^0$. (d) The K^+K^- invariant mass in $K^+K^-\pi^+\pi^-$. Filled circle with error bar: $\psi(3770)$ data, solid line: $\psi(3770) \rightarrow 2(\pi^+\pi^-)\pi^0$ or $K^+K^-\pi^+\pi^-$ Monte Carlo, dashed line: $\psi(3770) \rightarrow D\bar{D} \rightarrow 2(\pi^+\pi^-)\pi^0$ or $K^+K^-\pi^+\pi^-$ Monte Carlo, shaded histogram: $e^+e^- \rightarrow \gamma^* \rightarrow 2(\pi^+\pi^-)\pi^0$ or $K^+K^-\pi^+\pi^-$ from continuum data.

Event totals are shown for both the $\psi(3770)$ and the continuum in Table I, where $S_{\psi(3770)}$ (S_{co}) is the number of events in the signal region and $B_{\psi(3770)}$ (B_{co}) the number of events in the sideband region in $\psi(3770)$ (continuum) data. Also shown are yields for a $D\bar{D}$ Monte Carlo sample corresponding to 10 times the integrated luminosity of the data: $S_{D\bar{D}}$ ($B_{D\bar{D}}$) in the signal (sideband) region. Under the assumption that interference between $\psi(3770)$ decay and continuum production of the same final state is absent, the number of events

attributable to each $\psi(3770)$ decay mode, N_S , is

$$N_S = S_{\psi(3770)} - B_{\psi(3770)} - f_{\text{co}}(S_{\text{co}} - B_{\text{co}}) - f_{D\bar{D}}(S_{D\bar{D}} - B_{D\bar{D}}), \quad (1)$$

where f_{co} is mode dependent and listed in Table I, and $f_{D\bar{D}}=0.1$ is the scale factor for $D\bar{D}$ MC. Since no statistically significant excess is observed, we obtain a 90% C.L. upper limit on the number of events by adding 1.64 times the statistical uncertainty determined from the yields on the continuum and at the $\psi(3770)$.

The efficiency, ϵ , for each final state is obtained using a MC simulation [10] of the CLEO-c detector based on the EvtGen event generator [13]. No initial state radiation is included in the Monte Carlo, but final state radiation is accounted for. The efficiencies in Table I include the branching ratios for intermediate final states.

We correct the number of events by the efficiency ϵ , and normalize to the integrated luminosity \mathcal{L} to obtain the cross section:

$$\sigma = \frac{N_S}{\epsilon \mathcal{L}},$$

and normalize to the total number of the $\psi(3770)$ decays to obtain the branching ratio:

$$\mathcal{B} = \frac{N_S}{\epsilon N_{\psi(3770)}}.$$

The number of the $\psi(3770)$ decays is determined by $N_{\psi(3770)} = \sigma_{\text{tot}} \cdot \mathcal{L}$, where $\sigma_{\text{tot}} = (7.9 \pm 0.6)$ nb is the world average total cross section of the $\psi(3770)$ from [2].

The systematic uncertainties on the ratio of branching fractions share common contributions from the integrated luminosity (1.0%), uncertainty in f_{co} (10.0%), trigger efficiency (1.0%), and Monte Carlo statistics (2.0%). Other sources vary by channel. We include the following contributions for detector performance modeling quality: charged particle tracking (0.7% per track), $\pi^0/\eta(\rightarrow \gamma\gamma)$ finding (4.4%), Λ finding (3.0%), $\pi/K/p$ identification (0.3%/1.3%/1.3% per identified $\pi/K/p$), and scaled energy and mass resolutions (2.0%). The systematic uncertainty associated with the sideband background is obtained by coherently increasing the backgrounds both at the $\psi(3770)$ and on the continuum by one statistical sigma. Since the background in many modes is small, the Poisson probability for the observed number of background events to fluctuate up to the 68% C.L. value is calculated and interpreted as the uncertainty in the level of background. Many of the modes studied have resonant submodes, however the efficiencies do not differ by much. We generate MC data with a phase space model, and take a 10.0% uncertainty for decay model dependence. In the computation of the branching fractions, a common uncertainty of 7.6% enters due to the number of $\psi(3770)$ decays arising from the uncertainty in the total cross section of the $\psi(3770)$ [2]. We give the significance for each mode and upper limits (including the systematic error) for the cross section and branching ratio in Table I.

In summary we have searched for 25 exclusive multibody hadronic decay modes at the $\psi(3770)$. No significant signal is observed in any mode. For each mode we give the significance, and the upper limit on the cross section and branching fraction at 90% C.L. This study together with the $\psi(2S)$ multibody decay analysis [11] provide useful information about $S - D$ mixing. The cross section deficit remains a puzzle. However the uncertainty in the total cross section of the $\psi(3770)$ is large. A fine energy scan over the $\psi(3770)$ resonance to measure the total cross section would be very valuable.

TABLE I: For each final state h the following quantities are given: the number of events in the signal region, $S_{\psi(3770)}$, and background from sidebands, $B_{\psi(3770)}$, in $\psi(3770)$ data; the number of events in the signal region, S_{co} , and background from sidebands, B_{co} , in continuum data; the scale factor, f_{co} ; the number of events in the signal region, $S_{D\bar{D}}$, and background from sidebands, $B_{D\bar{D}}$, in a $D\bar{D}$ MC sample corresponding to 10 times the integrated luminosity of the $\psi(3770)$ data sample; the number of events attributable to $\psi(3770)$ decay, N_S , computed according to Eq. 1; the significance, in units of standard deviations; the efficiency, ϵ ; the cross section upper limit including the systematic error (90% C.L.), and the branching ratio upper limit including the systematic error (90% C.L.). For $\eta 3\pi$, the two decays modes $\eta \rightarrow \gamma\gamma$ ^a and $\eta \rightarrow 3\pi$ ^b are combined on line $\eta 3\pi$. (The sign of the significance indicates an excess/deficit of events).

mode	continuum		f_{co}	$10 \times D\bar{D}$ MC		$\psi(3770)$		N_S	Sig.	ϵ	σ U.L.	\mathcal{B} U.L.
h	S_{co}	B_{co}		$S_{D\bar{D}}$	$B_{D\bar{D}}$	$S_{\psi(3770)}$	$B_{\psi(3770)}$		($\#\sigma$)		(pb)	(10^{-4})
$2(\pi^+\pi^-)$	1471	28	2.49	1	13	3411	90	-266.5	-2.5	0.4305	8.7	11.2
$2(\pi^+\pi^-)\pi^0$	350	18	2.26	15	14	647	18	-120.5	-2.6	0.1990	8.2	10.6
$\eta\pi^+\pi^-$	15	0	2.57	0	0	41	1	1.5	0.1	0.0450	9.7	12.4
$\omega\pi^+\pi^-$	43	9	2.35	0	0	107	18	9.1	0.5	0.1638	4.6	6.0
$\eta 3\pi$ ^a	27	2	2.61	8	0	67	11	-10.1	-0.6	0.0688	4.5	5.8
$\eta 3\pi$ ^b	20	9	2.64	2	1	62	23	9.8	0.6	0.0248	24.0	30.7
$\eta 3\pi$											10.9	13.4
$\eta' 3\pi$	1	0	2.75	1	0	5	0	2.2	0.4	0.0149	19.2	24.4
$K^+K^-\pi^+\pi^-$	954	25	2.40	32	7	2262	47	-16.8	-0.2	0.3720	7.0	9.0
$\phi\pi^+\pi^-$	33	13	2.43	0	0	77	25	3.3	0.2	0.1629	3.2	4.1
ϕf_0	12	5	2.49	0	2	32	15	-0.2	0.0	0.0863	3.5	4.5
$K^+K^-\pi^+\pi^-\pi^0$	634	18	1.73	30	21	1121	32	24.9	0.5	0.1283	18.4	23.6
ηK^+K^-	3	0	2.50	0	0	3	0	-4.5	-0.7	0.0389	3.2	4.1
ωK^+K^-	62	12	2.31	0	1	114	14	-15.3	-0.7	0.1269	2.6	3.4
$2(K^+K^-)$	100	11	2.67	9	1	267	7	21.7	0.7	0.3170	4.6	6.0
ϕK^+K^-	46	15	2.59	4	0	118	22	15.2	0.7	0.1564	5.9	7.5
$2(K^+K^-)\pi^0$	20	0	2.88	8	0	50	0	-8.4	-0.6	0.1479	2.2	2.9
$p\bar{p}\pi^+\pi^-$	337	28	2.47	0	0	851	60	28.6	0.5	0.5149	4.5	5.8
$p\bar{p}\pi^+\pi^-\pi^0$	204	9	2.58	0	0	604	16	85.4	2.1	0.2259	14.4	18.5
$\eta p\bar{p}$	2	1	2.62	0	0	4	2	-0.6	-0.1	0.0469	4.2	5.4
$\omega p\bar{p}$	26	4	2.58	0	0	54	5	-7.8	-0.5	0.1421	2.2	2.9
$p\bar{p}K^+K^-$	25	1	2.62	0	0	89	3	23.0	1.5	0.4111	2.5	3.2
$\phi p\bar{p}$	2	3	2.69	0	0	2	2	0.0	0.0	0.1872	1.1	1.3
$\Lambda\bar{\Lambda}$	4	1	2.69	0	0	6	0	-2.1	-0.3	0.2154	1.0	1.2
$\Lambda\bar{\Lambda}\pi^+\pi^-$	23	4	2.37	0	0	42	7	-10.0	-0.7	0.1019	2.0	2.5
$\Lambda\bar{p}K^+$	65	7	2.57	0	0	150	11	-10.0	-0.4	0.2602	2.2	2.8
$\Lambda\bar{p}K^+\pi^+\pi^-$	29	3	2.64	0	0	94	17	8.2	0.4	0.1471	4.9	6.3

We gratefully acknowledge the effort of the CESR staff in providing us with excellent luminosity and running conditions. This work was supported by the National Science Foun-

dation and the U.S. Department of Energy.

- [1] S. Eidelman *et al.* (Particle Data Group), Phys. Lett. B **592**, 1 (2004).
- [2] J. Rosner, arXiv:hep-ph/0405196.
- [3] Q. He *et al.* (CLEO Collaboration), Phys. Rev. Lett. **95**, 121801 (2005).
- [4] J. Z. Bai *et al.* (BES Collaboration), Phys. Lett. B **605**, 63 (2005).
- [5] N. E. Adam *et al.* (CLEO Collaboration), arXiv:hep-ex/0508023.
- [6] R. A. Briere *et al.* (CLEO-c/CESR-c Taskforces & CLEO-c Collaboration), Cornell University LEPP Report No. CLNS 01/1742 (2001) (unpublished).
- [7] Y. Kubota *et al.* (CLEO Collaboration), Nucl. Instrum. Methods Phys. Res., Sect. A **320**, 66 (1992); D. Peterson *et al.*, Nucl. Instrum. Methods Phys. Res., Sect. A **478**, 142 (2002); M. Artuso *et al.*, Nucl. Instrum. Methods Phys. Res., Sect. A **554**, 147 (2005);
- [8] G. Crawford *et al.* (CLEO Collaboration), Nucl. Instrum. Methods Phys. Res., Sect. A **345**, 429 (1994).
- [9] C. M. Carloni Calame *et al.*, Nucl. Phys. B, Proc. Suppl. **131**, 48 (2004).
- [10] Computer code GEANT 3.21, in R. Brun *et al.*, CERN Report No. W5013, (1993) (unpublished).
- [11] R. A. Briere *et al.* (CLEO Collaboration), Phys. Rev. Lett. **95**, 062001 (2005).
- [12] As charged particle momentum resolution is excellent, a kinematically constrained fit only significantly improves the $\psi(3770)$ mass resolution for final state particles that decay to all neutral final states.
- [13] D.J. Lange, Nucl. Instrum. Methods Phys. Res., Sect. A **462**, 152 (2001).